Eur Spine J
DOI 10.1007/s00586-017-5234-0

CASE REPORT

# Design of mulitlevel OLF approach ("V"-shaped decompressive laminoplasty) based on 3D printing technology

**Qinjie Ling[1] · Erxing He[2] · Hanbin Ouyang[1] · Jing Guo[2] · Zhixun Yin[2] · Wenhua Huang[1]**

Received: 18 January 2017 / Revised: 25 April 2017 / Accepted: 19 July 2017


**Abstract**
*Purpose* To introduce a new surgical approach to the multilevel ossification of the ligamentum flavum (OLF) aided by three-dimensional (3D) printing technology.
*Methods* A multilevel OLF patient (male, 66 years) was scanned using computed tomography (CT). His saved DICOM format data were inputted to the Mimics14.0 3D reconstruction software (Materialise, Belgium). The resulting 3D model was used to observe the anatomical features of the multilevel OLF area and to design the surgical approach. At the base of the spinous process, two channels were created using an osteotomy bilaterally to create a "V" shape to remove the bone ligamentous complex (BLC). The decompressive laminoplasty using mini-plate fixation was simulated with the computer. The physical model was manufactured using 3D printing technology. The patient was subsequently treated using the designed surgery.
*Result* The operation was completed successfully without any complications. The operative time was 90 min, and blood loss was 200 ml. One month after the operation, neurologic function was recovered well, and the JOA score was improved from 6 preoperatively to 10. Postoperative CT scanning showed that the OLF was totally removed, and the replanted BLC had not subsided.
*Conclusion* 3D printing technology is an effective, reliable, and minimally invasive method to design operations. The technique can be an option for multilevel OLF surgical treatment. This can provide sufficient decompression with minimum damage to the spine and other intact anatomical structures.

**Keywords** 3D printing · Ossification of the ligamentum flavum · Decompressive laminoplasty

Co-first author: Erxing He

✉ Wenhua Huang
13822232749@139.com

Qinjie Ling
kmjw1982@163.com

Erxing He
heerxing717@163.com

Hanbin Ouyang
185729824@qq.com

Jing Guo
gjspine@163.com

Zhixun Yin
yzhixun@163.com

[1] Institute of Clinical Anatomy, School of Basic Medical Sciences, Southern Medical University, 1838 Guangzhou Avenue North, Guangzhou 510515, China

[2] Spinal Surgery, The First Affiliated Hospital of Guangzhou Medical University, 151 Yanjiang West Road, Guangzhou 510120, China

## Introduction

We designed a new approach for multilevel OLF ("V"-shaped decompressive laminoplasty) using 3D printing technology. The approach can not only achieve adequate decompression, but can also maintain the stability of the spine.

## Materials and methods

### Patient data

A 66-year-old man with OLF presented with gait disturbance. His feet had been numb for 2 years. The conservative

Published online: 27 July 2017

**Fig. 1** CT image showing the OLF located at T10–T12

treatment was invalid. The symptoms were worse, and he was not able to walk more than 45 yards. On admission, he could walk independently, but his gait was slow and unsteady. His muscle strength in the lower limbs was grade III, and his feet had hypoaesthesia. Hyperreflexia was not present at the bilateral patellar, ankle clonus, or Achilles tendon. The Japanese Orthopaedic Association score (JOA) was 6. The CT showed that his spinal cord was compressed by OLF at T10–T12. All the levels in OLF were the lateral type in the Miyakoshi categorization [1].

### 3D model and simulation

The patient's spine was scanned using CT (Siemens, Somatom Definition AS 128). The layer was 1 mm thick with a total of 946 mm. The data, in DICOM format, were inputted to the Mimics14.0 3D reconstruction software (Materialise, Belgium). The images showed the OLF in the T10–T12 area (Fig. 1); therefore, the images were re-sliced to save computational time. According to the bone boundary geometry, the thresholding range was set from 187 to 1309 Hu, and each layer was edited to distinguish between the bone and other surrounding tissues, such as muscle and ligament. The 3D model was reconstructed using images of the spine. We trimmed and smoothed the model, such that the model could be successfully printed. The information from the OLF, such as the location, size, and boundary, was clear (Fig. 2). Simulating the "V"-shaped decompressive laminoplasty at the base of the spinous process of T10–T12 confirmed the osteotomy side and angle (Fig. 3).

### Printing model and practice

The spine model and the BLC model were outputted in STL format, and both were processed using a 3D printer (Shanghai Pulicheng Electromechanical Technology Co. Ltd. Pulisheng Rui 400). A liquid photosensitive resin was solidified and formed under the action of an ultraviolet laser. The 3D physical models were printed in this manner (Fig. 4). We observed the physical model, performed the preoperative exercise, simulated the "V"-shaped lamina osteotomy, removed the OLF, and replanted the BLC with mini-plate (Double Medical Technology Inc., Xiamen City, China) fixation for the laminoplasty.

## Surgical technique

### Anaesthesia and position

After the general anaesthesia, the patient was placed in the prone position. His abdomen was suspended in mid-air to avoid putting pressure on the abdominal aorta. The motor

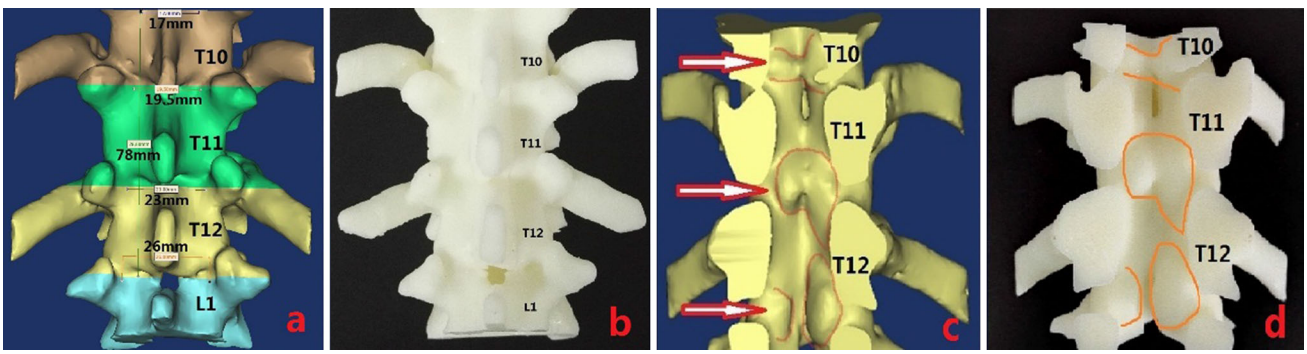


**Fig. 2** Spine anatomical information: **a** width of T10–T12 lamina, **b** rear view from the 3D printed model, **c** coronal image with the OLF geometry, and **d** coronal view from the 3D printed model (*arrow* the position of the OLF)

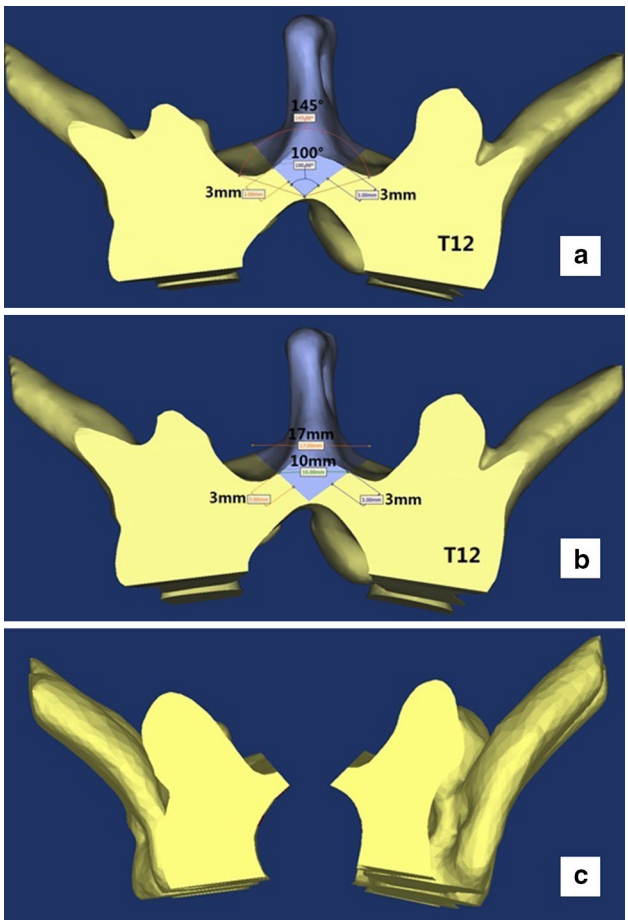


**Fig. 3** Surgical design: **a** range of the osteotomy angle, **b** range of the osteotomy width, and **c** virtual osteotomy effect map

evoked potentials (MEPs) were measured to monitor the spine cord.

### "V"-shaped lamina osteotomy

A skin incision was made at the T10–T12 levels in the middle line of the back, and the spinous process, the bilateral lamina, and the articular were exposed. The supraspinous ligament and inter-spinous ligament of T9–T10 and T12–L1 were cut. An oblique osteotomy was performed on the bilateral lamina at the base of the spinous process using a sharp chisel. The range was from the lower margin of the T12 lamina to the upper edge of the T10 lamina (Fig. 5a). The width of the osteotomy was approximately 16 mm. The "V"-shaped design made the osteotomy lines meet at the base of the spinous process. The "V" bottom from the spinal posterior margin was approximately 1 mm. The spinal canal was not broken through. The osteotomy was completed by the strength of the bone chisel, and elevating the BLC was performed with Kocher pliers. At that time, both the sides of the lamina formed a V-shaped bone groove, and the BLC and its base

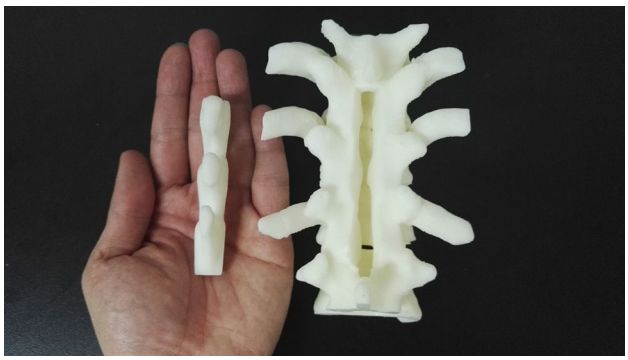

**Fig. 4** 3D printing 1:1 physical model used to simulate the osteotomy

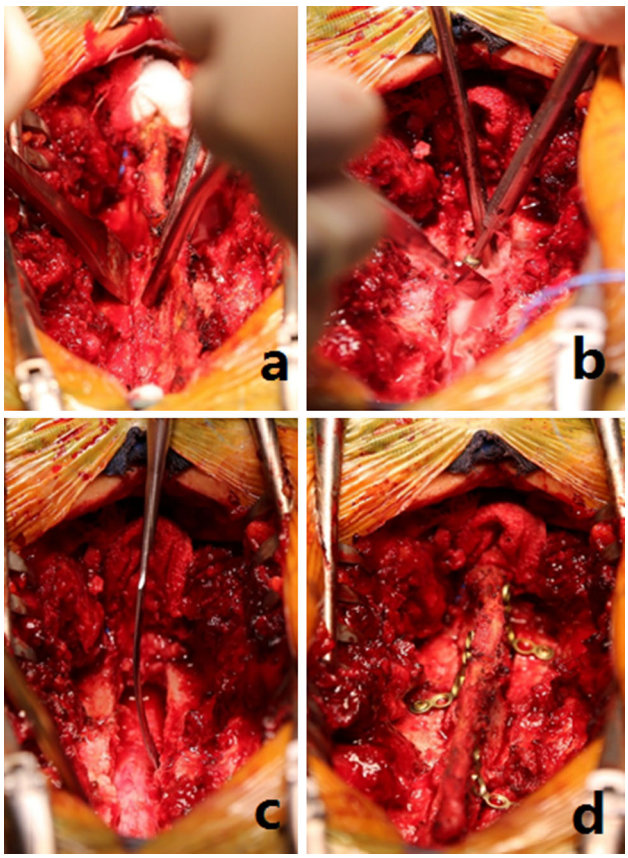


**Fig. 5** Intraoperative photographs: **a** oblique osteotomy, **b** decompression using a high-speed drill under the protection of a nerve dissector, **c** verifying the spinal canal, and **d** laminoplasty with miniplates

were cutoff. The cutoff was handled by a second assistant to remove the inside ossification bone for the replantation.

### Decompression

The V-shaped osteotomy groove bottom (normal spinal canal) was opened carefully with a small curette and small lamina rongeur breaking through the yellow ligament and

into the spinal canal. This was performed using a nerve dissector to protect the dural membrane and to separate it along the bone groove direction. The remaining spinous process was removed later. The bone groove opening was kept V-shaped during the process to, in particular, not damage the outer lamina, and an oblique surface of at least 3 mm was maintained. We carefully separated the OLF and the dural membrane with a small curette or a nerve dissector. Ossification of the dura was not found in the operation. Under the protection of the spatula plane of the nerve dissector, the thickened inside lamina and osseous ligament were removed with a high-speed drill (Fig. 5b). The spinal dura remained intact and the spinal canal was enlarged. After full decompression, we found that the spinal cord had a good pulse (see Fig. 5c).

### Laminoplasty

The treated BLC was replanted in situ with mini-plates for the lamina fixation. After suturing the supraspinous ligament of T9–T10 and T12–L1, the laminoplasty was completed (Fig. 5d).

## Results

The operation held for 90 min, and the blood loss was approximately 200 ml. Steroid, dehydration, and nerve nutrition drugs were used for the subsequent 3 days. The day after the operation, the drainage tube was removed, and the patient could walk by himself the next day. He was discharged within a week after the rescanned CT showed that decompression was acceptable (Fig. 6). A month later, he returned to the hospital by himself with a smile. His lower limb muscles and gait were improved significantly. The JOA score improved to 10 compared with the preoperative score of 6.

## Discussion

In 1999, D'Urso et al. [2] first used 3D printing technology for spinal surgery. Then, this technique became more and more popular. The main applications were the following: (1) modelling for planning and training [3–10]; (2) printing pedicle screw guide templates [11–16]; (3) customizing implants [17–25]; and (4) engineering bone [26–31]. In our opinion, the most helpful for surgeons is in assisting individual operation design as 3D printing technology is not yet mature.

The main strategy of the OLF surgical treatment is to achieve spinal nerve decompression through spinal osteotomy to remove the hyperplasia of the ossified tissue

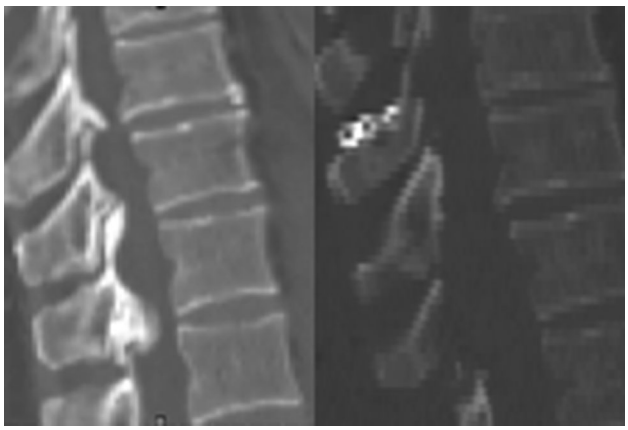

**Fig. 6** Preoperative and postoperative CT images

[32, 33]. Spinal osteotomy is a complex surgery. Incorrect or insufficient osteotomy can lead to poor results. However, there have only been a few detailed reports of spinal preoperative osteotomy planning. Many articles have shown 3D printed models and the postoperative pictures, but the processes of the surgical plan were not included [3–5, 8–10, 34]. A large number of clinical research results [33, 35–39] show that removal of too much spinal canal structure will cause instability, scar adhesion, and even re-compression of the nerve tissue. Therefore, under the premise of full decompression, retaining the original structure and function of the spine has been a subject of OLF in surgical treatment.

We used 3D printing technology to design a multi-level OLF approach. This provided detailed, stereoscopic, and intuitive spine anatomical information and tactile feedback to improve our understanding of the complexity of the spinal pathology (Fig. 2). In this case, the T10–L1 lamina thickness was observed to be gradually thinner (Fig. 7). The thinnest section of the lamina (at the base of the T12 spinous process upper edge) was the best choice for the design, because it was also safe in terms of the laminar osteotomy. Preoperative operations using the physical model made failure predictable, which helped us adjust the procedure to improve the surgical design. After trials, we found that the size of the osteotomy angle influenced the support of the BLC and the convenience decompression with the micro-drill (Fig. 8). The results of the simulation showed that the range of the "V"-shaped angle of the spinous process base was between 100° and 145° (a greater angle resulted in a greater supporting surface provided by the bevel) (Fig. 3a), and the width could be selected to be between 10 and 17 mm (Fig. 3b). We, therefore, left the outer lamina bevel at 1, 2, 3, ,4 and 5 mm, and found that 3 mm was the best option (Fig. 3). This design provided sufficient support for the BLC and space for

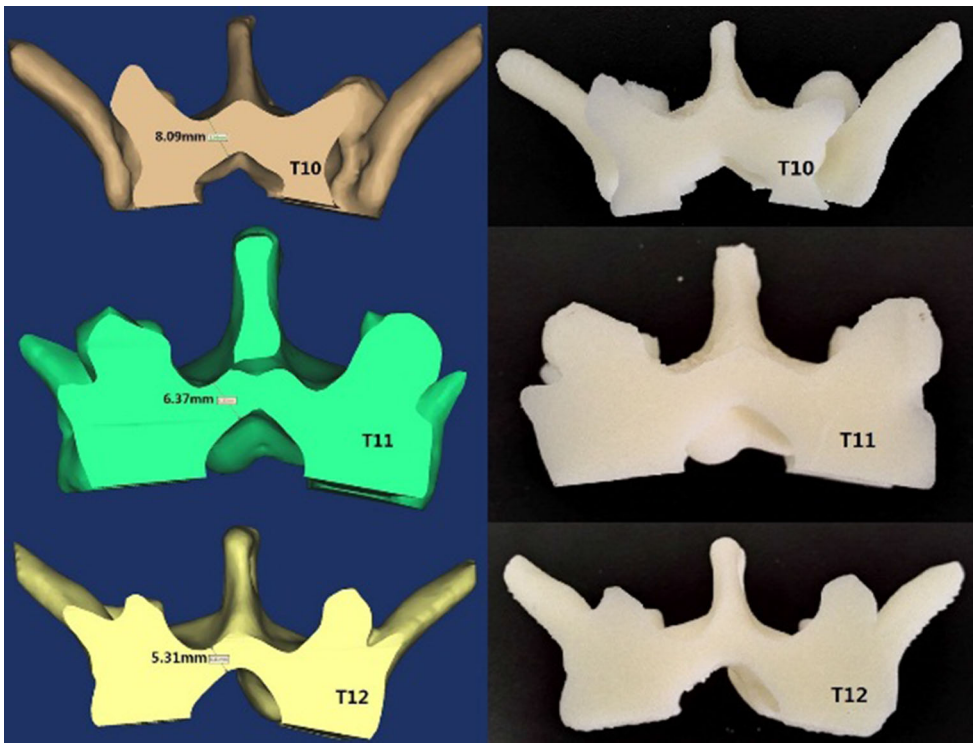


**Fig. 7** Image from the computer and the 3D printed model: thickness of the T10–T12 lamina

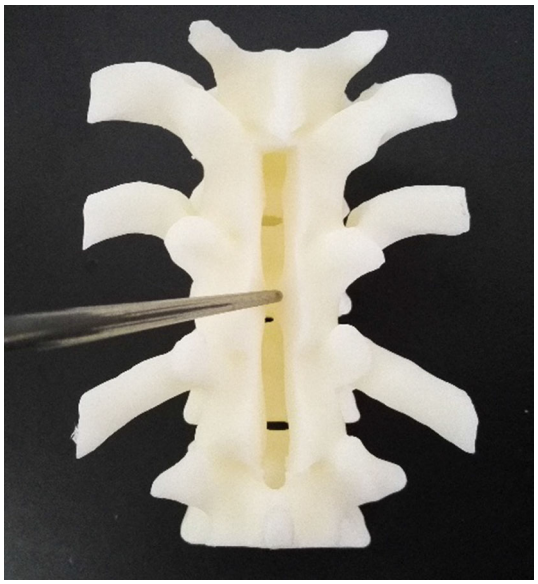

**Fig. 8** Simulating the decompression using a high-speed drill after the osteotomy

decompression. A maximum angle could not be used, because the articular process was blocked. We decided to use a length of 78 mm, a width of 16 mm, and a 120° angle as the osteotomy range for the surgery. The cut-off BLC could perfectly match the surrounding geometry of the structure (Fig. 4). The anatomy and biomechanics were restored.

The design of the multilevel OLF approach ("V"-shaped decompressive laminoplasty) based on 3D printing technology has the following advantages:

1. The base of the spinous process is thick enough for osteotomy. Bilateral bevels provide a good support plane for replantation. Avoiding the bone loss can be achieved using high-speed drill slotting, so the bone ligament complex did not collapse into the spinal canal or lead to compression.
2. The decompression area is visible. Even with the adhesion or dural ossification situation, there was sufficient space to operate using the floating method [40].
3. The original anatomical structure was retained. Due to the difference in the thickness of each lamina, the base of the cut-off BLC was serrated. Therefore, the replanted complex was hard to shift. There was no need to fix the mini-plate in each spinous process. This is good in terms of bone healing and restoring spinal stability.
4. The replantation provides a mechanical barrier to the spinal cord, effectively preventing scar formation and secondary compression [41, 42].
5. The retention of the spinous process provides an attachment for the back muscle tissue, which can effectively prevent muscle atrophy after surgery.
6. The immediate stability of the spine can shorten the time in bed and hospitalization and reduce patient cost.

## Conclusion

The design of a multilevel OLF approach based on 3D printing technology can be achieved in patients with multilevel OLF. 3D printing technology is an effective, reliable, and more minimally invasive method to design an operation.

**Acknowledgements** We would like to thank Mr Liao for the computer software support (Guangzhou You Dao Computer Technology Co., Ltd) and all the operating room staff. This work was supported by the Science and Technology Project of Guangdong Province (2014B090901055, 2015B010125005, and 2016B090917001), the south wisdom valley innovation team plan (2015CXTD05), and the National Natural Science Foundation of China (61427807).

**Compliance with ethical standards**

**Conflict of interest statement** None of the authors has any potential conflict of interest.

**Funding** The Science and Technology Project of Guangdong Province (2014B090901055, 2015B010125005, and 2016B090917001). South wisdom valley innovation team plan (2015CXTD05). National Natural Science Foundation of China (61427807).

## References

1. Miyakoshi N, Shimada Y, Suzuki T, Hongo M, Kasukawa Y, Okada K, Itoi E (2003) Factors related to long-term outcome after decompressive surgery for ossification of the ligamentum flavum of the thoracic spine. J Neurosurg 99(3 Suppl):251–256
2. D'Urso PS, Askin G, Earwaker JS, Merry GS, Thompson RG, Barker TM, Effeney DJ (1999) Spinal biomodeling. Spine 24(12):1247–1251
3. van Dijk M, Smit TH, Jiya TU, Wuisman PI (2001) Polyurethane real-size models used in planning complex spinal surgery. Spine 26(17):1920–1926
4. Izatt MT, Thorpe PL, Thompson RG, D'Urso PS, Adam CJ, Earwaker JW, Labrom RD, Askin GN (2007) The use of physical biomodelling in complex spinal surgery. Eur Spine J 16(9):1507
5. Paiva WS, Amorim R, Bezerra DA, Masini M (2007) Aplication of the stereolithography technique in complex spine surgery. Arq Neuropsiquiatr 65(2b):443–445
6. Yamazaki M, Okawa A, Akazawa T, Koda M (2007) Usefulness of 3-dimensional full-scale modeling for preoperative simulation of surgery in a patient with old unilateral cervical fracture-dislocation. Spine 32(18):E532–E536
7. Madrazo I, Zamorano C, Magallón E, Valenzuela T, Ibarra A, Salgadoceballos H, Grijalva I, Francobourland RE, Guízarsahagún G (2009) Stereolithography in spine pathology: a 2-case report. Surg Neurol 72(3):272–275
8. Mao K, Wang Y, Xiao S, Liu Z, Zhang Y, Zhang X, Wang Z, Lu N, Shourong Z, Xifeng Z (2010) Clinical application of computer-designed polystyrene models in complex severe spinal deformities: a pilot study. Eur Spine J 19(5):797–802
9. Yang JC, Ma XY, Lin J, Wu ZH, Zhang K, Yin QS (2011) Personalised modified osteotomy using computer-aided design–rapid prototyping to correct thoracic deformities. Int Orthop 35(12):1827–1832
10. Yang M, Li C, Li Y, Zhao Y, Wei X, Zhang G, Fan J, Ni H, Chen Z, Bai Y (2015) Application of 3D rapid prototyping technology in posterior corrective surgery for Lenke 1 adolescent idiopathic scoliosis patients. Medicine 94(8):e582
11. Wu ZX, Huang LY, Sang HX, Ma ZS, Wan SY, Cui G, Lei W (2011) Accuracy and safety assessment of pedicle screw placement using the rapid prototyping technique in severe congenital scoliosis. J Spinal Disord Tech 24(7):444
12. Kawaguchi Y, Nakano M, Yasuda T, Seki S, Hori T, Kimura T (2012) Development of a new technique for pedicle screw and Magerl screw insertion using a 3-dimensional image guide. Spine 37(23):1983–1988
13. Lu S, Zhang YZ, Wang Z, Shi JH, Chen YB, Xu XM, Xu YQ (2012) Accuracy and efficacy of thoracic pedicle screws in scoliosis with patient-specific drill template. Med Biol Eng Comput 50(7):751–758
14. Merc M, Drstvensek I, Vogrin M, Brajlih T, Recnik G (2013) A multi-level rapid prototyping drill guide template reduces the perforation risk of pedicle screw placement in the lumbar and sacral spine. Arch Orthop Trauma Surg 133(7):893–899
15. Kaneyama S, Sugawara T, Sumi M, Higashiyama N, Takabatake M, Mizoi K (2014) A novel screw guiding method with a screw guide template system for posterior C-2 fixation: clinical article. J Neurosurg Spine 21(2):231–238
16. Putzier M, Strube P, Cecchinato R, Lamartina C, Hoff E (2014) A new navigational tool for pedicle screw placement in patients with severe scoliosis: a pilot study to prove feasibility, accuracy, and identify operative challenges. J Spinal Disord Tech
17. Lin CY, Wirtz T, LaMarca F, Hollister SJ (2007) Structural and mechanical evaluations of a topology optimized titanium interbody fusion cage fabricated by selective laser melting process. J Biomed Mater Res, Part A 83(2):272–279. doi:10.1002/jbm.a.31231
18. Hunt J (2010) Truss implant. US
19. Beer ND, Merwe AVD (2013) Patient-specific intervertebral disc implants using rapid manufacturing technology. Rapid Prototyp J 19(2):8
20. Figueroa O, Rodríguez C, Siller H, Martínez-Romero O, Flores-Villalba E, Díaz-Elizondo J, Ramírez R (2013) Lumbar cage design concepts based on additive manufacturing, vol 102
21. Domanski J, Skalski K, Grygoruk R, Mróz A (2015) Rapid prototyping in the intervertebral implant design process. Rapid Prototyp J 21(6)
22. Knutsen AR, Borkowski SL, Ebramzadeh E, Flanagan CL, Hollister SJ, Sangiorgio SN (2015) Static and dynamic fatigue behavior of topology designed and conventional 3D printed bioresorbable PCL cervical interbody fusion devices. J Mech Behav Biomed Mater 49:332–342
23. Serra T, Capelli C, Toumpaniari R, Orriss IR, Leong JJ, Dalgarno K, Kalaskar DM (2016) Design and fabrication of 3D-printed anatomically shaped lumbar cage for intervertebral disc (IVD) degeneration treatment. Biofabrication 8(3):035001
24. Spetzger U, Frasca M, König SA (2016) Surgical planning, manufacturing and implantation of an individualized cervical fusion titanium cage using patient-specific data. Eur Spine J 25(7):1–8
25. Xu N, Wei F, Liu X, Jiang L, Cai H, Li Z, Yu M, Wu F, Liu Z (2016) Reconstruction of the upper cervical spine using a personalized 3D-printed vertebral body in an adolescent with Ewing sarcoma. Spine 41(1):50–54
26. Leukers B, Gülkan H, Irsen SH, Milz S, Tille C, Schieker M, Seitz H (2005) Hydroxyapatite scaffolds for bone tissue engineering made by 3D printing. J Mater Sci Mater Med 16(12):1121–1124
27. Khalyfa A, Vogt S, Weisser J, Grimm G, Rechtenbach A, Meyer W, Schnabelrauch M (2007) Development of a new calcium phosphate powder-binder system for the 3D printing of patient specific implants. J Mater Sci Mater Med 18(5):909–916

28. Lan PX, Jin WL, Seol YJ, Cho DW (2009) Development of 3D PPF/DEF scaffolds using micro-stereolithography and surface modification. J Mater Sci Mater Med 20(1):271–279
29. Whatley BR, Kuo J, Shuai C, Damon BJ, Wen X (2011) Fabrication of a biomimetic elastic intervertebral disk scaffold using additive manufacturing. Biofabrication 3(1):015004
30. Liu FH (2012) Synthesis of bioceramic scaffolds for bone tissue engineering by rapid prototyping technique. J Sol-Gel Sci Technol 64(3):704–710
31. Rosenzweig DH, Carelli E, Steffen T, Jarzem P, Haglund L (2015) 3D-printed ABS and PLA scaffolds for cartilage and nucleus pulposus tissue regeneration. Int J Mol Sci 16(7):15118–15135
32. Hirabayashi H, Ebara S, Takahashi J, Narasaki K, Takahara K, Murakami G, Kato H (2009) Surgery for thoracic myelopathy caused by ossification of the ligamentum flavum. J Korean Neurosurg Soc 46(3):189–194
33. Ben HK, Jemel H, Haouet S, Khaldi M (2003) Thoracic myelopathy caused by ossification of the ligamentum flavum: a report of 18 cases. J Neurosurg 99(2 Suppl):157–161
34. Li C, Yang M, Xie Y, Chen Z, Wang C, Bai Y, Zhu X, Li M (2015) Application of the polystyrene model made by 3-D printing rapid prototyping technology for operation planning in revision lumbar discectomy. J Orthop Sci 20(3):475–480
35. Okada K, Oka S, Tohge K, Ono K, Yonenobu K, Hosoya T (1991) Thoracic myelopathy caused by ossification of the ligamentum flavum. Clinicopathologic study and surgical treatment. Spine 16(3):280–287
36. Yonenobu K, Ebara S, Fujiwara K, Yamashita K, Ono K, Yamamoto T, Harada N, Ogino H, Ojima S (1987) Thoracic myelopathy secondary to ossification of the spinal ligament. J Neurosurg 66(4):511–518
37. Kurosa Y, Yamaura I, Nakai O, Shinomiya K (1996) Selecting a surgical method for thoracic myelopathy caused by ossification of the posterior longitudinal ligament. Spine 21(12):1458–1466
38. Chang UK, Choe WJ, Chung CK, Kim HJ (2001) Surgical treatment for thoracic spinal stenosis. Spinal Cord 39(7):362–369
39. Tanaka Y, Sato T, Aizawa T (2006) Surgery for ossification of the ligamentum flavum. Springer, Berlin
40. Miyashita T, Ataka H, Tanno T (2013) Spontaneous reduction of a floated ossification of the ligamentum flavum after posterior thoracic decompression (floating method); report of a case (abridged translation of a primary publication). Spine J: Off J North Am Spine Soc 13(8):e7–e9. doi:10.1016/j.spinee.2013.02.013
41. Lawson KJ, Malycky JL, Berry JL, Steffee AD (1991) Lamina repair and replacement to control laminectomy membrane formation in dogs. Spine 16(6 Suppl):222–226
42. Yücesoy K, Karci A, Kiliçalp A, Mertol T (2000) The barrier effect of laminae: laminotomy versus laminectomy. Spinal Cord 38(7):442–444. doi:10.1038/sj.sc.3101029